MINDO/3 calculation of the electronic structure of silicon nitride

V. A. Gritsenko and Yu. N. Novikov

Institute of Semiconductor Physics, Siberian Branch of the Russian Academy of Sciences, 630090 Novosibirsk, Russia

Yu. N. Morokov

Institute of Computer Technologies, Siberian Branch of the Russian Academy of Sciences, 630090 Novosibirsk, Russia

(Submitted October 14, 1996; resubmitted February 11, 1997)
Fiz. Tverd. Tela (St. Petersburg) **39**, 1342–1347 (August 1997)

The electronic structure of silicon nitride has been calculated by the semiempirical quantumchemical method MINDO/3 in the cluster approximation. The effect of cluster size and of boundary conditions on the partial density of one-electron states is analyzed. The results of the calculation are compared with experimental data on amorphous silicon nitride. The origin of a peak in the upper part of the valence band, which is seen in the Si$\mathbf{L}_{2,3}$ spectrum but not reproduced in the calculations is discussed. © *1997 American Institute of Physics.* [S1063-7834(97)00708-9]

The interest in studies of the amorphous silicon nitride (a-Si_3N_4) originates from its widespread use in electronics[1]. It exhibits a memory effect, i.e. it captures injected electrons and holes with a enormous delocalization rime. The nature of the deep centers responsible for the localization of electrons and holes in a-Si_3N_4 remains, however, unclear.[2–10]

Most of the preceding band-structure calculations of silicon nitride[11–18] made use of non-self-consistent methods. However, the same time it appears essential to take into account self-consistency in calculations of charge-transfer systems. A self-consistent version of the density functional method was employed in Ref. 19. The nonempirical MO LCAO approach was used to calculate the electronic structure of defects in Si_3N_4 in cluster approximation[20]. The latter study considered, however, a very small $Si(NH_2)_4$ cluster, which raises the question of the effect of boundary conditions on the results of calculations.

1. ELECTRONIC SPECTRUM CALCULATION AND THE CLUSTER STRUCTURE

We used the semiempirical quantumchemical method MINDO/3 (Ref. 21). MINDO/3 includes two two-center parameters (α_{AB} and B_{AB}) for description of the bonds coupling atoms A and B. No MINDO/3 parameters for the Si–N bond are available in the literature. In the present work, these parameters were found from a fit to experimental values for the bond length and dissociation energy of the SiN molecule.[22] The values $\alpha_{\mathrm{SiN}}=1.053011$ and $B_{\mathrm{SiN}}=0.434749$ thus obtained were used in subsequent calculations. An additional analysis showed that variation of these parameters does not lead to a noticeable improvement in the calculated band-edge positions for silicon nitride.

Unless otherwise specified, this paper presents graphs of partial one-electron densities-of-states (PDS) at the central Si (or N) atom and the nearest-neighbor N (or Si) atom. The discrete cluster levels were broadened by means of a Gaussian with a halfwidth of 0.5 eV. The energies were reckoned from the energy of the electron in vacuum. The experimental band-edge positions were determined by extrapolating x-ray emission and photoelectron spectra of a-Si_3N_4.[23]

A comparison of Si$\mathbf{L}_{2,3}$ spectra of amorphous and crystalline Si_3N_4 in the α and β phases indicates that the densities of Si $3s(3d)$ states in these phases do not differ.[24] This implies that the PDS is determined, in a first approximation, by short-range order in the atomic arrangement. We carried out calculations for clusters representing fragments of crystalline β-Si_3N_4 (space group $P6_3/m$). The geometric structure of amorphous Si_3N_4 was studied in Refs. 25 and 26.

Dangling bonds at the cluster boundary were terminated by hydrogen atoms. We divided the clusters into three groups according to the bonds they had at the boundary, namely, N clusters (N–H bonds only), S clusters (Si–H bonds only), and U clusters (both N–H and Si–H bonds).

The clusters studied in this work are depicted schematically in Fig. 1. Table I presents the numbers of Si–N bonds and of SiH_n and NH_n fragments in the clusters under study. The $S13$, $N46$, and $U90$ clusters are centered on the nitrogen atom, and the $N13$ and $S46$ clusters, on the silicon atom. In the $N46$ cluster, all nitrogen atoms, except for the central one, are bonded to the hydrogens. Similarly, all silicon atoms in $S46$, except for the central one, are also bonded to the hydrogen atoms. In contrast to the $N13$ and $S13$ clusters, $N46$ and $S46$ contain six-membered closed rings. In $U90$, only three out of 24 silicon atoms have the correct SiN_4 coordination. At the same time only 15 out of 27 nitrogen atoms have correct NSi_3 coordination.

2. COMPARISON OF THEORY WITH EXPERIMENT

Figure 2 compares the PDS's calculated for the $N13$ and $S13$ clusters with the experimental ones obtained for a-Si_3N_4 (Ref. 23). Also shown below is an x-ray photoelectron (XPS) spectrum of the valence band[23] with the inelastic-scattering background subtracted. The experimental and calculated PDS's in Fig. 2 and the subsequent figures are normalized to the maximum value (separately for the valence and conduction bands).

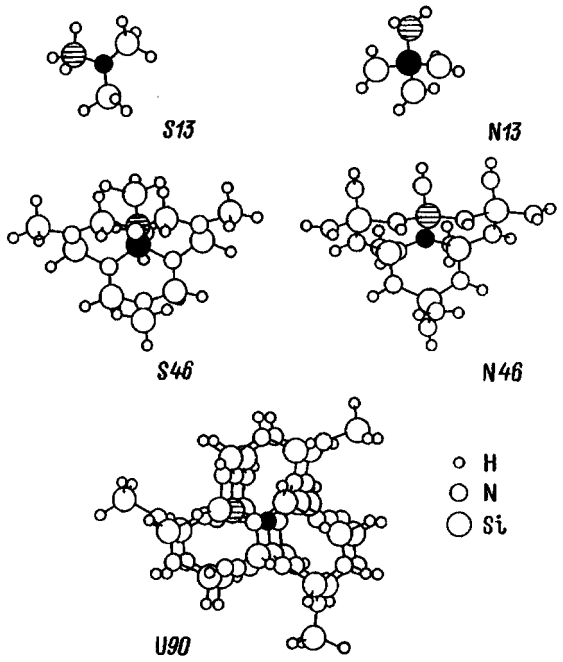

FIG. 1. Diagram of the clusters used in the calculations. The silicon and nitrogen atoms near the cluster center for which the PDS calculations were made are shown in black.

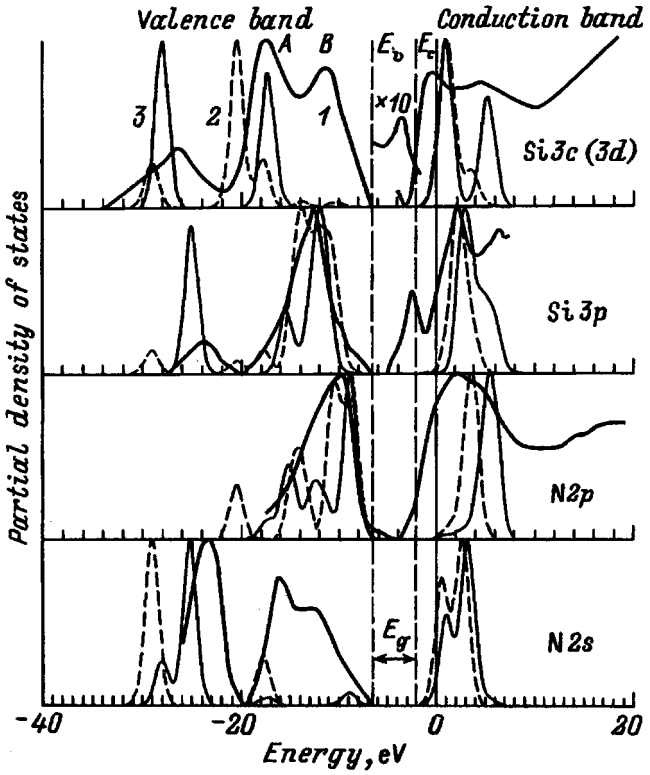

FIG. 2. Comparison of (*1*) experimental PDS for a-Si_3N_4 with calculations for (*2*) $S13$ and (*3*) $N13$ clusters. Shown below in this and subsequent figures is an XPS valence-band spectrum for a photon energy of 1486.6 eV after subtraction of the background due to inelastically scattered electrons.

These 13-atom clusters, small as they are, predict the existence of two valence bands. The lower one is formed primarily from nitrogen $2s$ states. The upper valence band derives from the N$2p$-,Si$3s, 3p$ bonding and N$2p_\pi$ nonbonding states. The wave functions of the N$2p_\pi$ states are oriented perpendicular to the NSi_3 plane. The calculations yield an overestimated band-gap width because of the smallness of the cluster. The bottom of the conduction band is formed from Si$3s$ and N$2s$ states.

The specific features of the silicon PDS are reproduced better in an $N13$ than an $S13$ cluster. This is explained by the fact that the silicon atom in $N13$ has the correct structure of the first coordination sphere. Calculations of the $N13$ cluster reproduce correctly the relative position of the Si$3s$ and Si$3p$ PDS's in the lower valence band. Note the absence of the experimentally observed peak B in the calculated Si $3s$ PDS close to the maximum of the upper valence band. While the nitrogen atom in $S13$ is bonded to three silicons, this does not improve the situation with the N$2s$ PDS compared to the $N13$ cluster.

Figure 3 presents experimental and calculated PDS's for the central atoms of nitrogen and silicon (and those closest to them) for the $N46$ and $S46$ clusters. The N$2s$ level splits at the central nitrogen in the $N46$ cluster into three peaks. The upper peak at an energy of -25 eV is close to the N$2s$ energy in Si_3N_4. The lower peak at about -32 eV is shifted relative to the maximum of the N$2s$ XPS peak by 8 eV. The

TABLE I. Number of Si–N bonds and of SiH_n and NH_n fragments in clusters.

Cluster	Formula	Si–N	SiH_1	SiH_2	SiH_3	NH_1	NH_2
$S13$	Si_3NH_{19}	3	0	0	3	0	0
$N13$	SiN_4H_8	4	0	0	0	0	4
$S46$	$Si_{12}N_7H_{27}$	21	0	6	5	0	0
$N46$	$Si_6N_{16}H_{24}$	24	0	0	0	6	9
$U90$	$Si_{24}N_{27}H_{39}$	69	18	0	3	12	0

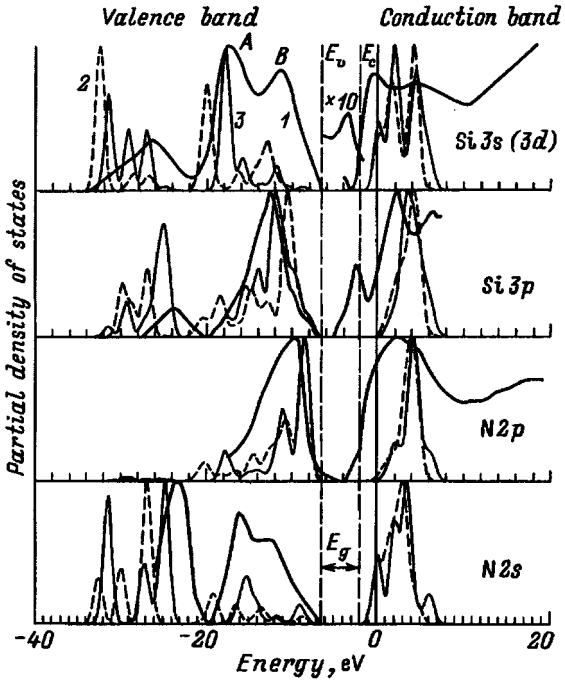

FIG. 3. Comparison of (*1*) experimental PDS for a-Si_3N_4 with calculations for (*2*) $S46$ and (*3*) $N46$ clusters.

splitting of the N2s peak into three features is due to the smallness of the cluster. An increase of cluster size should bring out other harmonics, which will eventually form the N 2s band. The large relative amplitude of the lower peak at -32 eV is due to the PDS being related to the central atom. In these conditions, the Si3s peak at -29 eV is formed by the wave function which vanishes at this atom because of symmetry. After summation over all nitrogen atoms, the relative amplitude of the lower peak at -32 eV in the N2s PDS decreased severalfold. The anomalously high lower peak in the lower Si3s PDS valence band calculated for the $S46$ cluster is of the same origin. The nitrogen atom in this cluster is not central, and therefore the lower peak in the N2s PDS has a substantially lower relative amplitude.

The Si3s and Si3p states of the lower valence band calculated for the $N46$ cluster are shifted with respect to one another in accordance with experiment. In the $S46$ cluster, all states in the lower valence band are shifted toward higher binding energies, and the overall agreement with experiment for this band is poorer than is the case with the $N46$ cluster.

The calculated N2p PDS's for $N46$ and $S46$ reproduce the general shape and width of the experimental PDS. The agreement of experiment with calculations for the Si3p PDS is worse for the $S46$ cluster than for the $N46$. The calculated peak is shifted relative to the experimental position by 1.5 eV.

The calculation of the Si3s PDS for the $N46$ cluster reproduces the position of peak A at -17 eV at the minimum of the upper valence band. The calculated amplitude of peak B lying at about -11 eV is, however, considerably lower than that obtained in experiment. The lower peak A in the upper valence band calculated for the $S46$ cluster is shifted by 2 eV compared to the experimental and calculated values for the $N46$.

Figure 4 shows the PDS's calculated for the $U90$ cluster. An increase in the number of atoms in the cluster is seen to produce the expected changes in the PDS. The bands become more clearly pronounced. At the same time the spectrum does not exhibit any significant features absent in the calculated patterns for the $N46$ and $S46$ clusters.

The charge transfer to the Si–N bonds obtained in this work, $\Delta q = 0.14e$, is one half the experimental value, $\Delta q = 0.30 \pm 0.05e$ (Refs. 2 and 23). MINDO/3 calculations of SiO_2 also yield an underevaluated charge transfer to the Si–O bonds.[27,28]

3. EFFECT OF BOUNDARY HYDROGEN ATOMS ON PDS

Hydrogen atoms terminating the dangling bonds at the cluster boundary approximate the effect of the nonexistent remainder of the crystal. For the Si, H, and N atoms, the Pauling electronegativity is 1.8, 2.1, and 3.0, respectively. Therefore if we look at the situation from the standpoint of correctly reproducing charge transport at cluster boundary, N–H bonds appear more reasonable to use than the Si–H bonds. On the whole, the results of the calculations confirm that N clusters reproduce better the electronic structure of silicon nitride than S clusters do.

Cluster calculations quite frequently consider PDS's averaged over all atoms of the corresponding species. This raises a question of the effect of boundary conditions on the accuracy of such a PDS. To analyze this effect, Fig. 5 presents PDS's for silicon and nitrogen atoms in $N46$ and $S46$ clusters averaged over all Si and all N atoms, respectively. A comparison with the PDS's in Fig. 3, which correspond only to the central atoms in the cluster, reveals a number of significant differences. On the whole, the averaged PDS's are seen to agree even better with experiment, than those calcu-

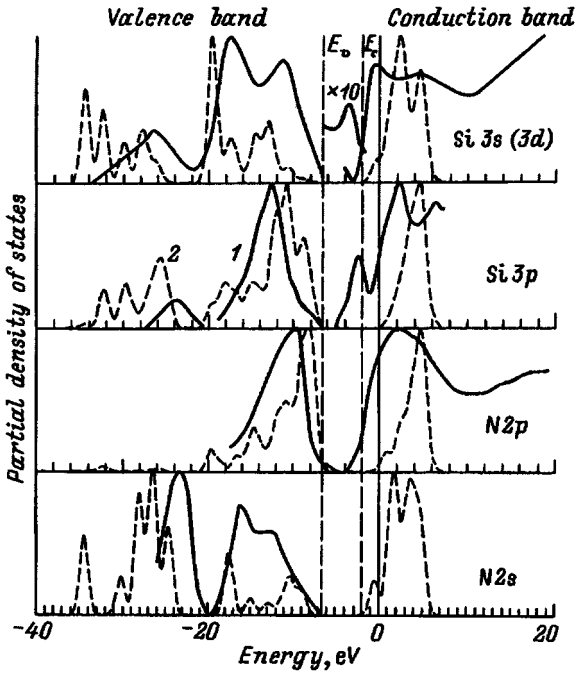

FIG. 4. Comparison of (*1*) experimental PDS for a-Si_3N_4 with (*2*) calculations for the $U90$ cluster.

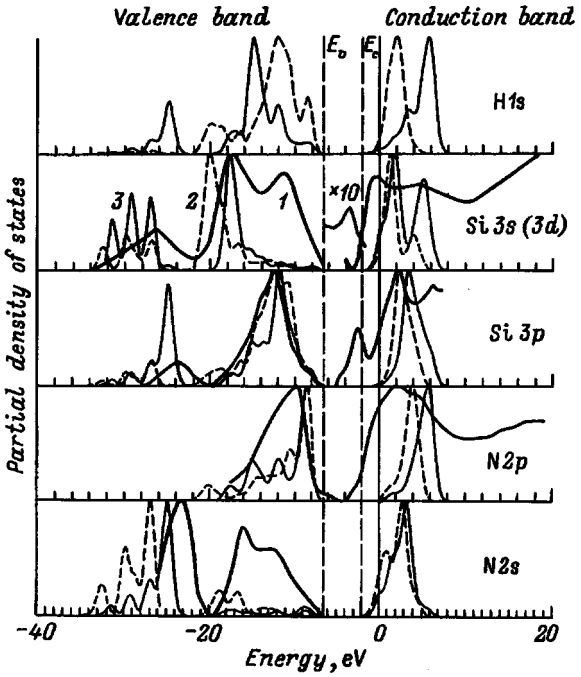

FIG. 5. PDS's for the $S46$ and $N46$ clusters averaged over all silicon and all nitrogen atoms, respectively. *1* — experiment, *2* — $S46$, *3* — $N46$.

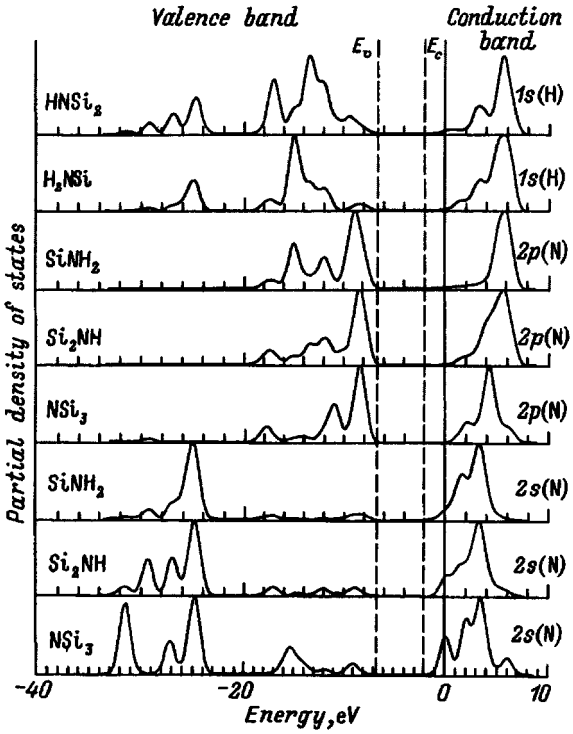

FIG. 6. PDS's for hydrogen and nitrogen atoms in the *N*46 cluster bound with different numbers of hydrogen atoms.

lated for the central atoms only (Fig. 3). This improvement is particularly evident for the N2p-PDS of the *S*46 cluster, and for the N2s-PDS of the *N*46. A more comprehensive analysis shows, however, that this improvement is largely fictitious and is due to the effect of the boundary hydrogen atoms.

The averaged N2p-PDS of the *N*46 cluster (Fig. 5) exhibits a noticeable peak at -15 eV. A comparison with the PDS averaged over hydrogen atoms, which is also shown in Fig. 5, shows that this peak originates from the formation of N–H bonds at cluster boundary. The improved agreement with experiment of the upper valence band of Si3s states for the *S*46 cluster is also probably associated with the formation of Si–H bonds at cluster boundary, which manifests itself in the H1s-PDS.

An analysis of the PDS's of peripheral nitrogen atoms (Fig. 6) permits a better understanding of the effect of hydrogen atoms. A comparison with the PDS's of hydrogens (the two upper graphs in Fig. 6) reveals, for example, that the peak at -15 eV in the averaged N2p-PDS of nitrogen obtained for the *N*46 cluster (Fig. 5) is due to the formation of NH_2 fragments at cluster boundary. An increase in the number of hydrogen atoms bonded to the silicon atom also results in a shift of the N2s-PDS toward the top of the lower valence band of the nitride. Therefore the improved agreement with experiment for the N2s-band, which is observed in the averaged N2s-PDS, originates from the shift of the PDS caused by interaction of the nitrogen with hydrogen atoms.

4. ASSIGNMENT OF THE Si$L_{2,3}$ SPECTRUM AND XPS SPECTRUM OF THE VALENCE BAND

In the dipole approximation, Si$\mathbf{L}_{2,3}$ emission spectra involves transitions from the Si3s and Si3d-states to the Si 2p- levels. Thus the renormalized Si$L_{2,3}$ spectrum represents actually a superposition of the Si3s and Si3d-PDS's. The experimental Si3s(3d)-PDS (Fig. 2) has two peaks (*A* and *B*) in the upper valence band. Peak *B* is lower in amplitude than peak *A* by about 20%.

The amplitude of peak *B* is quoted[29] to be about one half that of peak *A*. This discrepancy is accounted for[29] by the effect of fourth-order N*K* emission spectrum. This conjecture is, however, argued against by the fact that the maximum in the N*K* spectrum is shifted by 2 eV with respect to peak *B* toward the top of the valence band.[23,30–32] In addition, the Si$\mathbf{L}_{2,3}$ spectra, which are close to those shown in Fig. 2, are reported[20] to be obtained in conditions in which the intensity of the first-order NK_α spectrum was two orders of magnitude lower than that of the Si$\mathbf{L}_{2,3}$ spectrum. In these conditions, fourth-order NK_α emission practically cannot contribute to the Si$\mathbf{L}_{2,3}$ spectrum. Thus the reason for the difference in the relative amplitude of peak *B* in the Si$\mathbf{L}_{2,3}$ spectrum between the experimental data shown in Fig. 2 and those presented in Ref. 29 remains an open question.

The relative amplitude of peak *B* with respect to peak *A* in the Si3s-PDS observed experimentally is substantially in excess of the calculated value (Figs. 2–5). The calculations for the silicon nitride[6,15,20] and silicon dioxide[28,33–36] which take into account only the Si3s,3p-atomic orbitals exhibit a similar pattern.

Contributions from excess silicon are proposed as a possible reason for the large relative amplitude of peak *B* in the SiO_2 spectrum. Excess silicon can form in SiO_2 when the sample is irradiated by an electron beam to excite the Si$\mathbf{L}_{2,3}$-spectrum. A similar situation may arise when measuring a Si$\mathbf{L}_{2,3}$ spectrum in Si_3N_4. Electron beam irradiation of Si_3N_4 is accompanied by production of excess silicon.[37] Figure 7a and b shows Si$\mathbf{L}_{2,3}$ spectra of amorphous silicon[38] and of Si_3N_4 (Ref. 23) plotted with respect to the top of the valence band E_v. A comparison of these two spectra leads to the conclusion that their superposition cannot increase the relative amplitude of peak *B*. Figure 7c illustrates superposition of Si$\mathbf{L}_{2,3}$ spectra from Si_3N_4 and *a*-Si. Thus the presence of excess silicon cannot account for the large amplitude of peak *B* in the Si$\mathbf{L}_{2,3}$ spectrum of the silicon nitride.

Calculations[20] of Si_3N_4 predict a considerable contribution of Si3d orbitals near the top of the valence band. This prediction found support[29] based on the calculations of Ref. 12. A similar proposal received widespread interest as a way to interpret the *B* peak observed in the Si$\mathbf{L}_{2,3}$ spectrum of SiO_2 (Ref. 39). Calculations taking into account Si 3d-atomic states yield contradictory results. For example, some studies[33,35,40] do not indicate a noticeable contribution of Si3d-states to the valence band of SiO_2. Other results (see, for instance, Refs. 41 and 42), however, appear to demonstrate that the high-energy peak in Si$\mathbf{L}_{2,3}$ spectra of SiO_2 derives from the Si3d-orbitals. It appears natural to connect the contradictory conclusions concerning the effect of Si 3d-atomic functions with the ambiguity in the selection of

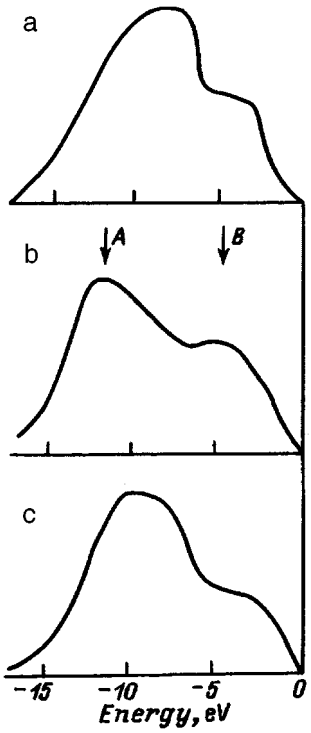

FIG. 7. Si$\mathbf{L}_{2,3}$ spectra of (a) amorphous silicon and (b) amorphous Si_3N_4; (c) superposition of spectra *a* and *b* in the 2:1 ratio.

the parameters of the Si3*d*-basis functions used.

Figures 2–5 display also an XPS spectrum of the Si_3N_4 valence band (after subtraction of the inelastic-scattering background), which can provide additional information on the contribution of the Si3*s* and Si3*d*-states. The photoionization cross-section ratio calculated for photons of energy 1486.6 eV incident on a free atom, is Si3*s*:Si3*p*:N2*s*:N2*p*=1:0.17:1.1:0.072 (Ref. 43). The photoionization cross section for Si3*d* atomic states is three orders of magnitude smaller than that for the Si3*s*-states,[44] and therefore the contribution of the former to the XPS spectra of the upper valence band may be neglected. If in a first approximation we neglect the contribution of Si3*p* and N2*p*-states to XPS spectra, then these spectra will reflect the distribution of the Si3*s* and N2*s*-states in the valence band of Si_3N_4. Since there is no experimental information on the partial density of N2*s*-states, one cannot consider the XPS data as supporting the assignment of peak *B* in the Si$\mathbf{L}_{2,3}$ spectrum to Si3*s*-orbitals. Moreover, the accuracy of the calculations is not high enough to permit separation of the Si3*s* from N2*s* contributions to the upper part of XPS spectra.

In view of the contradictory character of the calculated contributions of Si3*d*-states to the PDS of the upper valence band of Si_3N_4 and SiO_2, one can propose a more general interpretation of the large relative amplitude of peak *B* in the Si$\mathbf{L}_{2,3}$ spectrum of these materials. Namely, the Si$\mathbf{L}_{2,3}$ spectrum is formed by electronic transitions to the Si2*p*-states from delocalized bulk states, rather than from purely atomic states. Part of the contribution to peak *B* can be assigned to transitions from Si3*d*-states. The magnitude of this fraction will depend on the parameters of the Si3*d* atomic states used for interpretation of experimental data. The remainder can be attributed to one-center transitions from Si3*p*-states, if we assume that interaction with other atoms distorts the potential of these states, thus lifting the forbiddenness from optical transitions. These transitions can, in turn, be related also to other than one-center electronic transitions to Si2*p* from the N2*p* bonding atomic states of nearest-neighbor nitrogen atoms. This interpretation is argued for by the fact that peak *B* in the Si3*s*-PDS (Fig. 2) lies between the maxima in the Si 3*p* and N2*p*-PDS's.

The possible contribution to this part of the silicon nitride Si$\mathbf{L}_{2,3}$ spectrum of non-one-center electronic transitions from Si3*s*-states of nearest-neighbor silicon atoms was considered in Ref. 29. The probability of such transitions, estimated[29] by means of the Hermann-Skillman functions, was found to constitute 5–10% of that of the one-center Si–3*s*-Si2*p*-transitions. It is conceivable that the contribution of the N2*p*–Si2*p* nearest-neighbor two-center transitions is substantially larger. Thus the discrepancy between calculations and experiment with respect to peak *B* in the Si$\mathbf{L}_{2,3}$ spectrum of Si_3N_4 and SiO_2 can be removed if we assume the peak to result not only from Si3*s*,3*d*-states but from the Si3*p* and N2*p* bonding states as well.

In summary, we have performed a cluster study of the electronic structure of silicon nitride by the MINDO/3 quantumchemical method. Calculations of clusters ranging in size from 13 to 90 atoms have been carried out. The main features of the electronic structure of silicon nitride are shown to be seen already with 13-atom clusters. A comprehensive analysis of PDS's for clusters of different size has been made using Si–H and N–H bonds as boundary conditions. Local PDS's calculated for atoms close to cluster center are found to be more appropriate for analysis.

The discrepancy between theory and experiment with respect to the contribution of Si3*s*(3*d*)-states to the upper part of the valence band in silicon nitride and dioxide can be explained if we assume that peak *B* in the Si$\mathbf{L}_{2,3}$ spectrum is due not only to one-center transitions from Si3*s*,3*d*-states, but to two-center transitions from the N2*p* bonding states of the nearest-neighbor nitrogen atoms as well.

[1] V. I. Belyi, L. L. Vasilyeva, V. A. Gritsenko *et al.*, in *Silicon Nitride in Electronics* (Material Science Monographs, Vol. 34), edited by A. V. Rzhanov, (North-Holland, Amsterdam, 1988), p. 555.
[2] V. A. Gritsenko, *Structure and Electronic Spectrum of Amorphous Dielectrics in Silicon MIS Structures* [in Russian], Nauka, Novosibirsk (1993).
[3] S. Fujita and S. Sasaki, J. Electrochem. Soc. **132**, 398 (1985).
[4] P. A. Pundur, Yu. G. Shavalgin, and V. A. Gritsenko, Phys. Status Solidi A **94**, K107 (1986).
[5] P. M. Lenahan, D. T. Krick, and J. Kanicki, Appl. Surf. Sci. **39**, 392 (1989).
[6] J. Robertson, Philos. Mag. B **63**, 47 (1991).
[7] W. L. Warren, J. Kanicki, J. Robertson, E. H. Poindexter, and P. J. McWhorter, J. Appl. Phys. **74**, 4034 (1993).
[8] V. A. Gritsenko and P. A. Pundur, Fiz. Tverd. Tela (Leningrad) **28**, 3239 (1986) [Sov. Phys. Solid State **28**, 1829 (1986)].
[9] V. A. Gritsenko, E. E. Meerson, I. B. Travkov, and Yu. V. Goltvyanskiĭ, Mikroélektronika **16**, No. 1, 42 (1987).
[10] V. A. Gritsenko, Yu. P. Kostikov, and L. V. Khramova, Fiz. Tverd. Tela (Leningrad) **34**, 2424 (1992) [Sov. Phys. Solid State **34**, 1300 (1992)].
[11] R. J. Sokel, J. Phys. Chem. Solids **41**, 899 (1980).
[12] J. Robertson, Philos. Mag. B **44**, 215 (1981).
[13] S. Y. Ren and W. Y. Ching, Phys. Rev. B **23**, 5454 (1981).

[14] A. G. Petukhov, Fiz. Tverd. Tela (Leningrad) **27**, 95 (1985) [Sov. Phys. Solid State **27**, 55 (1985)].
[15] E. C. Ferreira and C. E. T. Gonçalves da Silva, Phys. Rev. B **32**, 8332 (1985).
[16] L. Martín-Moreno, E. Martínez, J. A. Vergés, and F. Yndurain, Phys. Rev. B **35**, 9683 (1987).
[17] J. Robertson, J. Appl. Phys. **54**, 4490 (1983).
[18] J. Robertson, Philos. Mag. B **69**, 307 (1994).
[19] Y. Xu and W. Y. Ching, Physica B **150**, 32 (1988).
[20] E. P. Domashevskaya, Yu. K. Timoshenko, V. A. Terekhov *et al.*, J. Non-Cryst. Solids **114**, 495 (1989).
[21] R. C. Bingham, M. J. S. Dewar, and D. H. Lo, J. Am. Chem. Soc. **97**, 1285 (1975).
[22] *Molecular Constants of Inorganic Compounds: a Handbook* [in Russian], edited by K. S. Krasnov, Khimiya, Leningrad (1979).
[23] V. A. Gritsenko and Yu. P. Kostikov, Fiz. Tverd. Tela (St. Petersburg) (in press).
[24] V. I. Nithianandam and S. E. Schnatterly, Phys. Rev. B **36**, 1159 (1987).
[25] E. A. Repnikova, V. A. Gurtov, and Z. V. Panova, Phys. Status Solidi A **119**, 113 (1990).
[26] K. Wakita, F. Makimura, and Y. Nakayama, J. Appl. Phys. **34**, 1425 (1995).
[27] A. H. Edwards and W. B. Fowler, J. Phys. Chem. Solids **46**, 841 (1985).
[28] V. A. Gritsenko, R. M. Ivanov, and Yu. N. Morokov, Zh. Éksp. Teor. Fiz. **108**, 2216 (1995) [Sov. Phys. JETP **81**, 1208 (1995)].
[29] R. D. Carson and S. E. Schnatterly, Phys. Rev. B **33**, 2432 (1986).
[30] I. A. Brytov, V. A. Gritsenko, Yu. P. Kostikov, E. A. Obolenskiĭ, and Yu. N. Romashchenko, Fiz. Tverd. Tela (Leningrad) **26**, 1685 (1984) [Sov. Phys. Solid State **26**, 1022 (1984)].
[31] I. A. Brytov, E. A. Obolenskii, Yu. N. Romashenko, and V. A. Gritsenko, J. Phys. (Paris) **45**, C2-888 (1984).
[32] I. A. Brytov, V. A. Gritsenko, and Yu. N. Romashchenko, Zh. Éksp. Teor. Fiz. **89**, 562 (1985) [Sov. Phys. JETP **62**, 321 (1985)].
[33] J. R. Chelikowski and M. Schluter, Phys. Rev. B **15**, 4020 (1977).
[34] R. N. Nucho and A. Madhukar, Phys. Rev. B **21**, 1576 (1980).
[35] D. Lohez and M. Lannoo, Phys. Rev. B **27**, 5007 (1983).
[36] R. P. Gupta, Phys. Rev. B **32**, 8278 (1985).
[37] R. Hezel, Radiat. Eff. **65**, 101 (1982).
[38] V. A. Terekhov, N. M. Medvedev, V. M. Andreeshchev, V. M. Kashkarov, and É. P. Domashevskaya, Poverkhnost' No. 6, 91 (1984).
[39] D. L. Griscom, J. Non-Cryst. Solids **24**, 155 (1977).
[40] A. J. Bennett and L. M. Roth, J. Phys. Chem. Solids **32**, 1251 (1971).
[41] A. Simunek and G. Weich, J. Non-Cryst. Solids **137**/**138**, 903 (1991).
[42] I. Tanaka, J. Kawai, and H. Adachi, Phys. Rev. B **52**, 11733 (1995).
[43] J. J. Yeh and I. Lindau, Atomic Data-Nuclear Data Tables **32**, 1 (1985).
[44] G. K. Wertheim, in *Electron and Ion Spectroscopy of Solids*, edited by L. Fiermans, J. Vennik, and W. Dekeyser, Plenum Press, New York (1978), p. 195.

Translated by G. Skrebtsov